

Article

Performance and Long-Term Stability of Pd/PSS and Pd/Al₂O₃ Membranes for Hydrogen Separation

Simona Liguori¹, Adolfo Iulianelli¹, Francesco Dalena², Pietro Pinacci³, Francesca Drago³, Maria Broglia³, Yan Huang⁴ and Angelo Basile^{1,*}

¹ Institute on Membrane Technology of Italian National Research Council (ITM-CNR), c/o University of Calabria, Cubo 17/C, Rende (CS) 87036, Italy; E-Mails: s.liguori@itm.cnr.it (S.L.); a.iulianelli@itm.cnr.it (A.I.)

² Chemistry and Chemical Technologies Department, University of Calabria, Cubo 15/D, Via P. Bucci, Rende (CS) 87036, Italy; E-Mail: dalena.ch@gmail.com

³ RSE S.p.A., Via Rubattino 54, Milano (MI) 20134, Italy; E-Mails: pietro.pinacci@rse-web.it (P.P.); francesca.drago@rse-web.it (F.D.); maria.broglia@rse-web.it (M.B.)

⁴ State Key Laboratory of Materials-Oriented Chemical Engineering, College of Chemistry & Chemical Engineering, Nanjing University of Technology, Xin-Mo-Fan Road 5, Nanjing 210009, China; E-Mail: huangy@njut.edu.cn

* Author to whom correspondence should be addressed; E-Mail: a.basile@itm.cnr.it; Tel.: +39-(0)98-449-2013; Fax: +39-(0)98-440-1071.

Received: 20 December 2013; in revised form: 10 February 2014 / Accepted: 24 February 2014 / Published: 6 March 2014

Abstract: The present work is focused on the investigation of the performance and long-term stability of two composite palladium membranes under different operating conditions. One membrane (Pd/porous stainless steel (PSS)) is characterized by a ~10 µm-thick palladium layer on a porous stainless steel substrate, which is pretreated by means of surface modification and oxidation; the other membrane (Pd/Al₂O₃) is constituted by a ~7 µm-thick palladium layer on an asymmetric microporous Al₂O₃ substrate. The operating temperature and pressure ranges, used for studying the performance of these two kinds of membranes, are 350–450 °C and 200–800 kPa, respectively. The H₂ permeances and the H₂/N₂ selectivities of both membranes were investigated and compared with literature data. At 400 °C and 200 kPa as pressure difference, Pd/PSS and Pd/Al₂O₃ membranes exhibited an H₂/N₂ ideal selectivity equal to 11700 and 6200, respectively, showing stability for 600 h. Thereafter, H₂/N₂ selectivity of both membranes progressively decreased and after around 2000 h, dropped dramatically to 55 and 310 for the Pd/PSS and

Pd/Al₂O₃ membranes, respectively. As evidenced by Scanning Electron Microscope (SEM) analyses, the pinholes appear on the whole surface of the Pd/PSS membrane and this is probably due to release of sulphur from the graphite seal rings.

Keywords: palladium composite membrane; porous stainless steel; ideal selectivity; hydrogen separation

1. Introduction

In recent years, the rise in the request for hydrogen in the petrochemical industries as well as for supplying fuel cells has led to ever increasing attention on the development of new and alternative methods for hydrogen separation/purification [1].

In this context, dense palladium membranes have received growing consideration owing to their complete selectivity towards hydrogen permeation with respect to all other gases. Indeed, an extensive literature has been reported on thick Pd unsupported membranes, which have been utilized and applied for producing high-grade hydrogen, although characterized by low permeability [1–3]. Recently, in order to enhance the hydrogen permeability, research has been focused on palladium thickness reduction, making possible simultaneously high mechanical resistance. Currently, the studies of scientists in this area are mainly devoted to the development of Pd-based composite membranes characterized by a thin metallic layer deposited onto porous substrates, showing such benefits as high hydrogen permeability, selectivity towards hydrogen permeation, and mechanical resistance [4–7]. Typical substrate materials for composite membranes are stainless steel and ceramics [8–12]. Stainless steel sintered porous supports are particularly suitable owing to good weldability and mechanical strength. They seem to be more convenient with respect to ceramic substrates for integration with Pd-based layers because of their thermal expansion coefficient being similar to Pd metal [13,14]. However, a porous stainless steel (PSS) support shows some drawbacks such as a high rough surface and a large and wide pore size, which cause some problems during membrane manufacture. Moreover, the long-term stability of these aforementioned composite membranes is affected by intermetallic diffusion, which occurs when the metallic layer is directly in contact with the porous support [15]. In order to avoid this phenomenon, different approaches, based on the use of an intermediate layer between metal and support, have been studied by various authors [16–19]. For instance, Shu *et al.* [16] have used an ultrathin (0.1 μm) intermediate layer of titanium nitride as diffusion barrier between a Pd/Ag alloy film and a PSS substrate. Nam and Lee [17] proposed silica layer utilization also for improving the structural stability of the membrane. Ma *et al.* [18] created an intermediate layer by *in situ* oxidation of the porous support. Recently, Wei *et al.* [19] reported an effective method for modifying the PSS substrate by using a pencil coating, forming a graphite layer as a diffusion barrier.

On the contrary, ceramic supports show some benefits, being chemically inert and stable over a wide temperature range [20,21]. Moreover, their structure presents essential properties for manufacturing defect-free membranes with thin metallic layers such as small pore sizes with uniform distribution. Nevertheless, in order to realize ceramic supports showing these characteristics, numerous coating and sintering steps are necessary with a consequent cost increase [22]. Therefore, low-cost

supports characterized by some defects are usually considered. In the latter case, prior to Pd-layer deposition, the support needs to be pre-treated either by Chemical Vapour Deposition (CVD) activation [5], or an Al₂O₃ suspension [23] or a sol-gel coating technique [21,24].

Numerous methods for depositing a thin Pd-layer onto porous supports have been investigated [25–31] and the technique most widely used is the electroless plating (ELP) owing to its various benefits [13,30,31]. Indeed, the hardness of the deposited layer and its strong adhesion to the support, the deposit uniformity on the complex geometry as well as the low preparation cost and the simplicity of the equipment and procedure can be considered as some of these benefits in the use of this technique [24,32].

Currently, the issue requiring to be overcome is related to the long-term stability of Pd-composite membranes under different operating conditions. To the best of our knowledge, there are few scientific papers dealing with the long-term test of Pd-based composite membranes [24,33–36]. For instance, Nair *et al.* [33] studied the permeating characteristics of Pd supported on alumina membrane, characterized by a 13 µm Pd-layer and reported a decrease of H₂/N₂ ideal selectivity after 300 h. Peters *et al.* [24] tested Pd–Ag supported on PSS in 50% H₂/N₂ at 19.6 bar for 2400 h at 350–450 °C and observed a gradual H₂/N₂ selectivity decrease from 3000 to 500. They attributed the leak growth to pinhole formation. Also Kulprathipanja *et al.* [35] observed a significant decrease in the H₂/N₂ ideal selectivity, testing 4 µm Pd–Cu supported onto a porous alumina membrane after 340 h. On the contrary, Yun *et al.* [36] reported a stable H₂/N₂ ideal selectivity of 9200 for 150 h at 460 °C by investigating an ultra-thin Pd composite membrane.

Consequently, the aim of this work is to evaluate the long-term stability, as well as estimating the life-time, of two different composite membranes, characterized by a thin Pd-layer supported onto alumina and PSS supports, under different operating conditions. Furthermore, comparisons with experimental data from the open literature are also made and further discussed.

2. Experimental

2.1. Membrane Preparation and Membrane Module Setup

Several methods have been developed for depositing a palladium layer onto porous substrates such as magnetron sputtering [25], spray pyrolysis [26], CVD [27,28], physical vapour deposition [29] and ELP [13,30,31]. In this work, ELP technique has been chosen for preparing both composite membranes owing to its important benefits such as the uniformity of the thin palladium layer, simplicity of the required equipment and low cost.

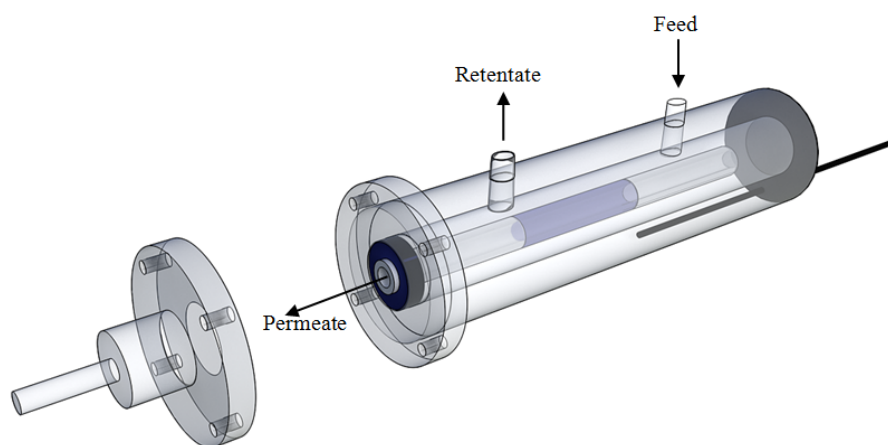
The first membrane consists of ~10 µm of Pd-layer deposited onto a PSS tubular support, with a mean pore size of about 2 µm and a porosity around 20%. The support was supplied by Mott Metallurgical Corporation (Farmington, MI, USA) having a 1.0 cm O.D. AISI 316L porous tube with a total length equal to 7.7 cm. The porous support was welded to two non porous AISI 316 L tubes (Industrial Welding Corporation, Manila, Philippines), one of which was closed.

This membrane was manufactured at RSE Spa (IT) laboratories and its preparation was carried out by using a similar procedure to Ma *et al.* [18]. This procedure consists of machine polishing of the support with a diamond paste to reduce surface roughness, support cleaning in an ultrasonic bath,

support oxidation in an oven with air at 500 °C, support activation and successive deposition of the Pd-layer by ELP [37,38]. After deposition, the Pd/PSS membrane presents an active area equal to 24.2 cm².

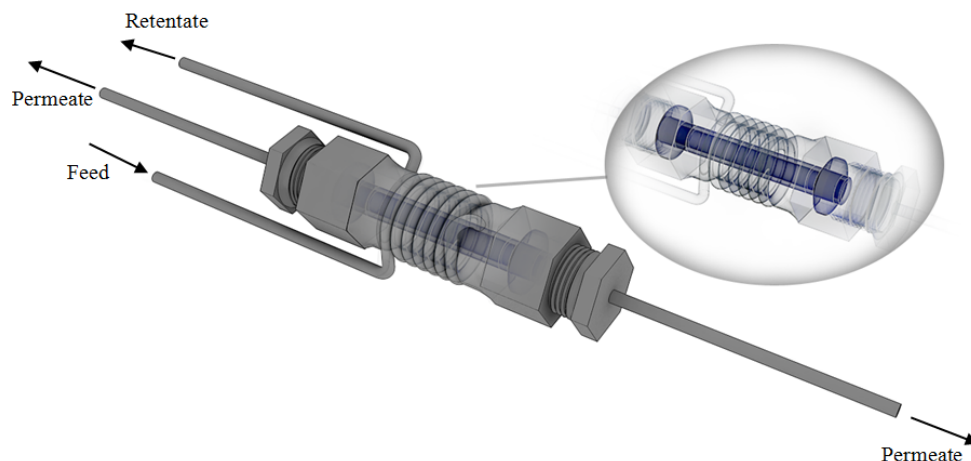
The membrane module, used for housing the aforementioned membrane, is shown in Figure 1 and consists of a tubular stainless steel module (length 280 mm, internal diameter (i.d.) 20 mm), in which a graphite o-ring avoids the mixing of permeate and retentate streams.

Figure 1. Scheme of membrane module housing the Pd/porous stainless steel (PSS) membrane.



The second membrane was manufactured at Nanjing University of Technology (Nanjing, China) by following the preparation procedure of Collins and Way [39]. It consists of ~7 μm Pd-layer deposited onto an Al₂O₃ support, supplied by Gao Q Funct. Mat. Company (Nanjing, China). The support shows a total length equal to 7.5 cm with an outer and inner diameter equal to 1.3 cm and 0.9 cm, respectively, and it is open at both ends. The active area of the Pd/Al₂O₃ membrane is about 17.2 cm². In this case, two graphite o-rings are used to ensure that the permeate and retentate streams are not mixed with each other. In Figure 2, the scheme of the Pd/Al₂O₃ membrane module is shown.

Figure 2. Scheme of membrane module housing the Pd/Al₂O₃ membrane.



2.2. Experimental Details

The experimental plant used for carrying out the long-term tests consists of: Brooks instruments 5850S mass-flow controllers, which regulate the gas feed flow rates, a membrane module and a bubble flow meter for measuring the gas permeating flux through the membrane. Both membranes were heated in a helium atmosphere. The investigated temperatures were in the range 350–450 °C for Pd/Al₂O₃ and 380–420 °C for Pd/PSS. The restricted processing temperature range of Pd/PSS is due to its temperature limits. In particular, the lower and upper temperature limits are 360 °C and 430 °C, respectively. The pressure in the retentate side was varied from 2.0 to 8.0 bar by means of a back pressure placed at the outlet side, while the pressure in the permeate side is kept constant at 1.0 bar without using any sweep gas.

The measurements are carried out for a period of around 2000 h.

Concerning the performance description of both Pd-based composite membranes, some equations have been defined as reported below:

$$\text{Ideal Selectivity } (\alpha_{\text{H}_2/i}) = \frac{\text{Permeance}_{\text{H}_2}}{\text{Permeance}_i} \quad (-) \quad (1)$$

$$\text{Permeance}_i = \frac{J_i}{\Delta p} \quad (\text{mol/Pa} \cdot \text{m}^2 \cdot \text{s}) \quad (2)$$

where i can be He, N₂, H₂, CH₄, CO₂; J_i the permeating flux of i -gas; and Δp the trans-membrane pressure.

3. Result and Discussion

3.1. Permeation Measurements

Permeation tests with pure gases such as H₂, N₂, He, CH₄, CO₂ have been performed in the range of 200–800 kPa, by using both Pd-based composite membranes. Firstly, the permeation tests were performed with He and N₂ for checking the presence of any defect in the palladium layer. In Figure 3, at 400 °C the permeance of N₂ and He for both membranes as a function of the trans-membrane pressure is reported.

It appears evident that the permeance of each gas is increased by increasing the trans-membrane pressure, showing that both membranes are affected by pinholes or defects. These imperfections can be caused, among others, by the decomposition of some impurities present in the ELP solution and co-deposited onto porous supports with palladium particles [12]. As a comparison at each trans-membrane pressure investigated, the Pd/PSS membrane showed lower He and N₂ permeance values than the Pd/Al₂O₃ membrane, illustrating that the first membrane is characterized by a lower presence of defects in the Pd-layer. The same behavior was found by carrying out the permeation tests with CH₄ and CO₂. Moreover as shown in Table 1, CO₂ and CH₄ permeances for both membranes are increased by increasing the trans-membrane pressure.

Figure 3. N₂ and He permeances as a function of trans-membrane pressure for both Pd-based membranes at T = 400 °C.

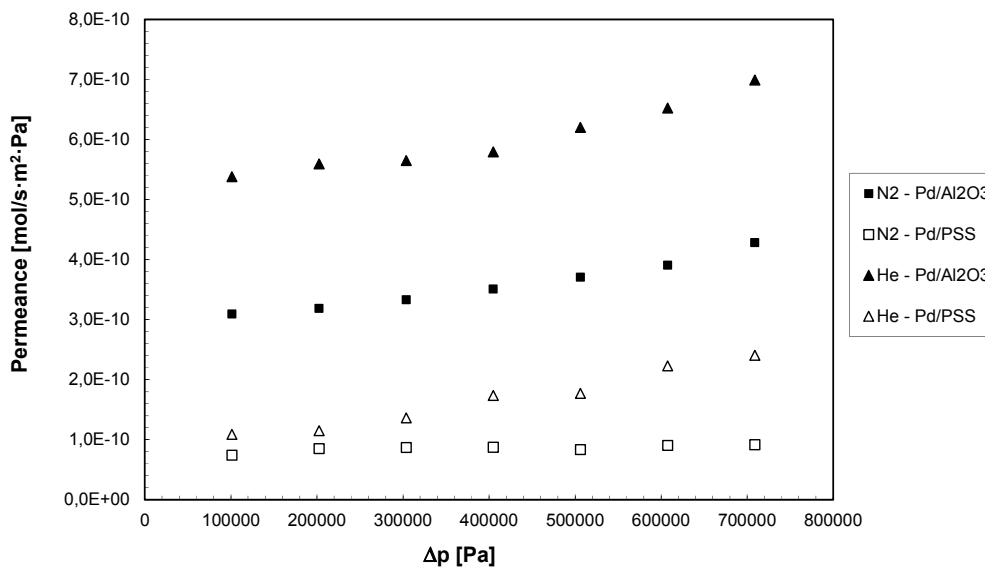


Table 1. CH₄ and CO₂ permeances as a function of the trans-membrane pressure difference for both Pd-based composite membranes at T = 400 °C.

Δp (Pa)	Pd/Al ₂ O ₃		Pd/PSS	
	CH ₄ Permeance	CO ₂ Permeance	CH ₄ Permeance	CO ₂ Permeance
	(mol/s·m ² ·Pa)	(mol/s·m ² ·Pa)	(mol/s·m ² ·Pa)	(mol/s·m ² ·Pa)
1.01 × 10 ⁵	6.27 × 10 ⁻¹⁰	7.28 × 10 ⁻¹⁰	2.73 × 10 ⁻¹⁰	3.52 × 10 ⁻¹⁰
2.02 × 10 ⁵	8.11 × 10 ⁻¹⁰	1.18 × 10 ⁻⁹	3.60 × 10 ⁻¹⁰	5.11 × 10 ⁻¹⁰
3.03 × 10 ⁵	9.91 × 10 ⁻¹⁰	1.36 × 10 ⁻⁹	4.01 × 10 ⁻¹⁰	5.75 × 10 ⁻¹⁰
4.04 × 10 ⁵	1.05 × 10 ⁻⁹	1.61 × 10 ⁻⁹	4.27 × 10 ⁻¹⁰	6.68 × 10 ⁻¹⁰
5.05 × 10 ⁵	1.09 × 10 ⁻⁹	1.68 × 10 ⁻⁹	4.46 × 10 ⁻¹⁰	7.08 × 10 ⁻¹⁰
6.06 × 10 ⁵	1.13 × 10 ⁻⁹	1.75 × 10 ⁻⁹	4.70 × 10 ⁻¹⁰	7.34 × 10 ⁻¹⁰
7.07 × 10 ⁵	1.17 × 10 ⁻⁹	1.86 × 10 ⁻⁹	4.89 × 10 ⁻¹⁰	7.41 × 10 ⁻¹⁰

As a further investigation, the influence of temperature was also evaluated for both membranes at Δp = 1.0 bar. In particular, for Pd/PSS and Pd/Al₂O₃ membranes the temperature was varied between 380–420 °C and 350–450 °C, respectively. As a result, N₂, He, CO₂ and CH₄ permeances are decreased by increasing temperature for both membranes. Therefore, as a global consideration, it was observed that, for each gas among He, N₂, CO₂ and CH₄, the permeance was increased almost linearly by increasing the trans-membrane pressure (Figure 3 and Table 1) and by decreasing the temperature (not shown), indicating that the pure gas permeation through the membrane takes place by Knudsen diffusion and viscous flow through the defects [40].

3.2. Hydrogen Permeation Test

Recently, hydrogen transport through dense Pd-layer membranes has been extensively studied and it has been considered as a complex process that, generally, takes place by a solution-diffusion mechanism, which involves several steps, such as mass transfer, surface-reactions, bulk diffusion, *etc.*

Generally, the hydrogen permeating flux through the membrane can be expressed by the following equation:

$$J_{H_2} = P \cdot (p_{\text{Retentate}}^n - p_{\text{Permeate}}^n) \quad (3)$$

where J_{H_2} is the hydrogen permeating flux through the membrane, P the hydrogen permeance, $p_{H_2\text{-retentate}}$ and $p_{H_2\text{-permeate}}$ are the hydrogen partial pressure in the retentate and permeate sides, respectively, and n the dependence factor of the hydrogen flux on the hydrogen partial pressure, generally in the range of 0.5–1. The n value is often used as an indicator for the rate-controlling step of the hydrogen permeation through the palladium (composite or not) membrane. Values equal to 0.5 (Sieverts-Fick's law) indicate that the diffusion of atomic hydrogen through the dense metal layer is the rate-limiting step.

Deviations from this value can be attributed to a several factors such as defects in the Pd-layer, palladium surface contamination or transport resistance of the substrate material. However, for a thin membrane (<1 μm) the surface-reaction is the controlling step and n is equal to 1.

The hydrogen permeance is influenced by temperature by the Arrhenius law:

$$P = P^\circ \cdot \exp(-Ea/RT) \quad (4)$$

where P° , Ea , R and T are the pre-exponential factor, apparent energy activation, universal gas constant and absolute temperature, respectively.

Generally, in order to establish the membrane permeation characteristics, P° , Ea and n need to be estimated. Therefore, in this work hydrogen permeation measurements at different temperature and trans-membrane pressure are required.

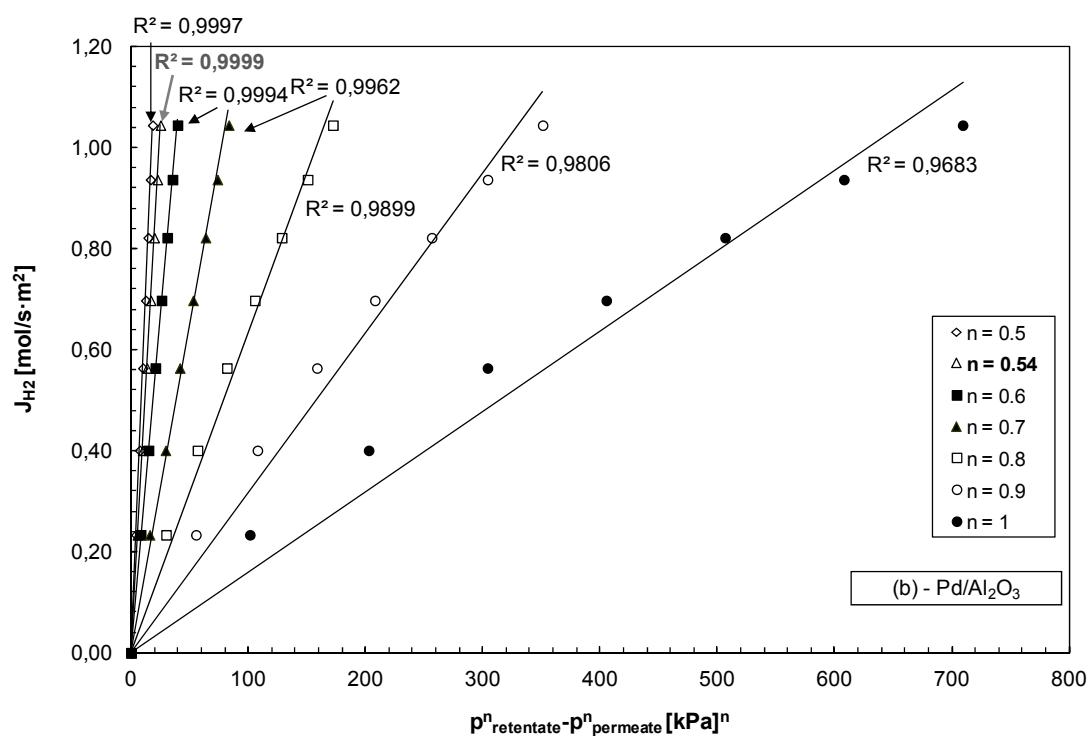
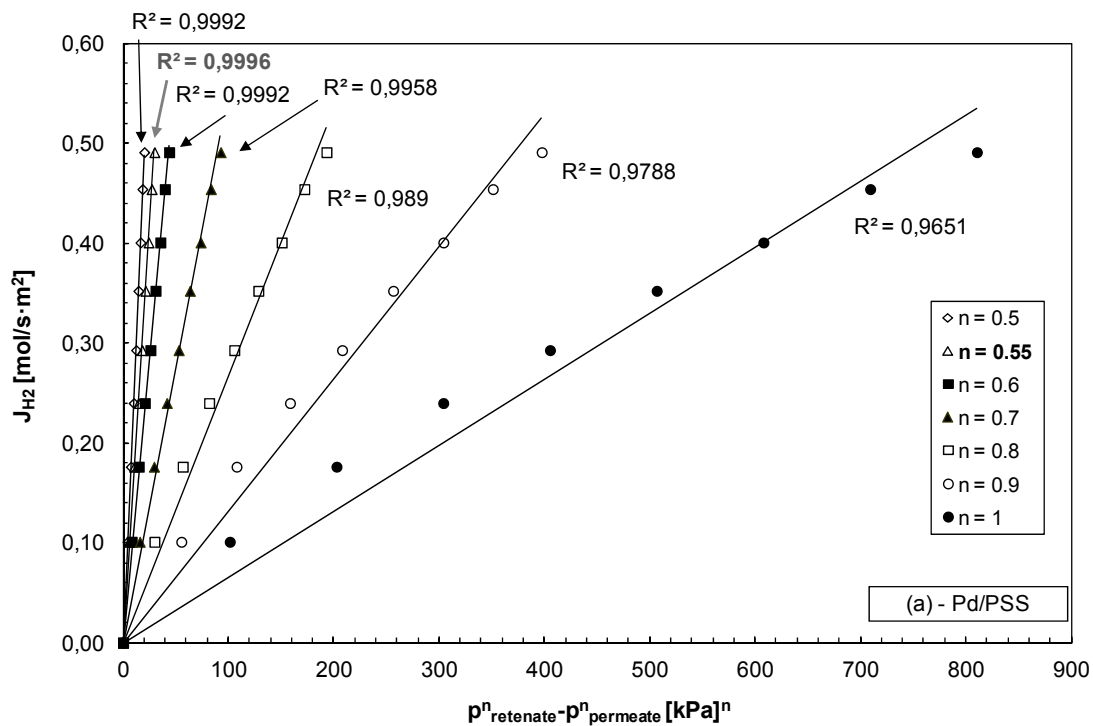
At 400 °C and by varying the trans-membrane pressure, hydrogen permeating flux through the Pd/PSS is shown in Figure 4a and through the Pd/Al₂O₃ membrane in Figure 4b by considering various “ n ” values. Depending on each “ n ” considered, the highest linear regression factors (R^2) were found to be $n = 0.55$ for Pd/PSS and $n = 0.54$ for Pd/Al₂O₃. Therefore, the transport of hydrogen through both composite membranes is mainly limited by diffusion through the palladium bulk. Nevertheless, the deviation from the 0.5 value suggests that hydrogen flux does not depend only on atomic diffusion through palladium, but is influenced by other factors such as the presence of impurities on the membrane surface which could hinder hydrogen dissociation [41].

Furthermore, as shown in Figure 5 the temperature was varied for estimating Ea and P° for both membranes by using an Arrhenius plot of the hydrogen permeance against the reciprocal temperature. As a result, Ea equal to 14.7 kJ/mol and 11.4 kJ/mol and P° equal to 6.85×10^{-6} mol/s·m²·Pa and 1.77×10^{-5} mol/s·m²·Pa were evaluated for Pd/PSS and Pd/Al₂O₃ membranes, respectively.

Table 2 summarizes a comparison between the Ea and n values determined in this work with respect to other similar data found in the specialized literature.

As shown, the values of Ea are in good agreement with those reported by other researchers. For instance, Wang *et al.* [42] found 7.1 kJ/mol, Tong *et al.* [43] detected 16.2 kJ/mol and Zahedi *et al.* [44] reported a similar value to the one obtained with the Pd/PSS membrane of this work by using a Pd composite supported onto PSS modified with WO₃. Regarding the n value, deviation from 0.5 was also found by other authors [31,39,43,45–48].

Figure 4. H₂ permeating flux as a function of the trans-membrane pressure at different “n” values; T = 400 °C, (a) Pd/PSS and (b) Pd/Al₂O₃ membrane.



(a)

(b)

Figure 5. Arrhenius plot for pure hydrogen permeation tests using Pd/PSS and Pd/Al₂O₃ membranes at $\Delta p = 1$ bar.

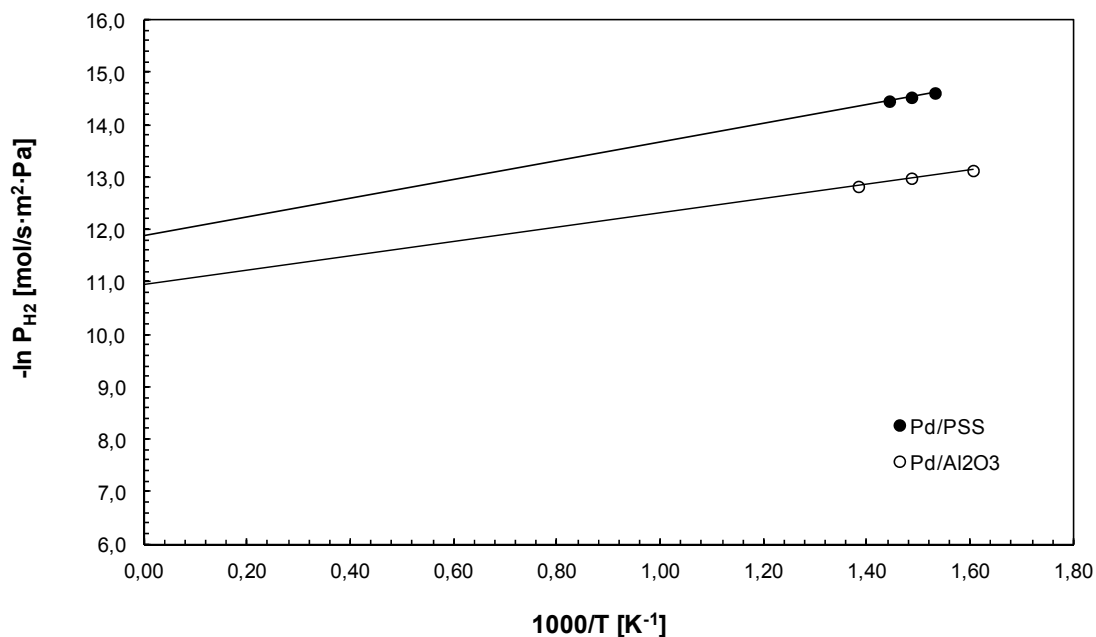


Table 2. Comparison of *Ea* and *n* values determined for both Pd/PSS and Pd/Al₂O₃ membranes with respect to similar data on Pd-based membranes reported in the literature.

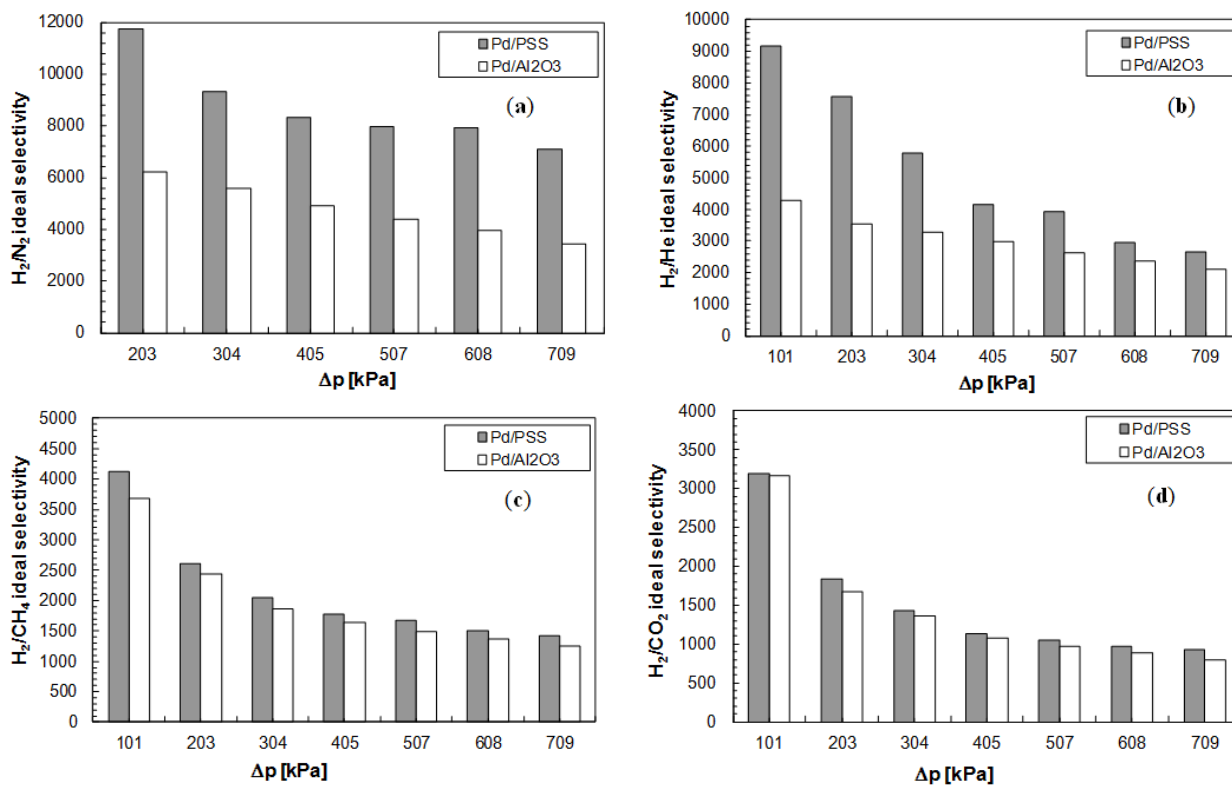
Membrane	Layer of Pd (μm)	<i>Ea</i> (kJ/mol)	<i>n</i>	References
Pd/WO ₃ /PSS	12	14.7	0.5	[44]
Pd/Al ₂ O ₃	8.5	5.7	0.778	[45]
Pd/ZrO ₂ /PSS	10	7.1	0.5	[42]
Pd/CeO ₂ /PSS	6	17.3	0.85	[43]
Pd/Al ₂ O ₃	11.4	8.9	0.58	[39]
Pd/SiO ₂ /PSS	6	24 ^a	1	[46]
Pd/FeCr/PSS	11	15.03	0.5	[49]
Pd/Al ₂ O ₃	4.5	18.3	1	[47]
Pd/Al ₂ O ₃	5	7.0	1	[31]
Pd/MPSS	20	16.4	0.60	[48]
Pd/Al ₂ O ₃ /PSS	15	20.6	0.5	[7]
Pd/PSS	10	14.7	0.55	This work
Pd/Al ₂ O ₃	7	11.4	0.54	This work

^a Calculations based on permeation data in the literature.

3.3. Membrane Performance

By considering the permeance values at different trans-membrane pressures of each aforementioned gas, it is possible to evaluate the performance of both Pd-based membranes in terms of hydrogen over the other gases ideal selectivities. Figure 6a–d reports the comparison of the ideal selectivities as a function of trans-membrane pressure for both Pd/PSS and Pd/Al₂O₃ membranes at *T* = 400 °C.

Figure 6. Ideal selectivities as a function of the trans-membrane pressure at $T = 400\text{ °C}$ for Pd/PSS and Pd/Al₂O₃ membranes. (a) $\alpha_{\text{H}_2/\text{N}_2}$; (b) $\alpha_{\text{H}_2/\text{He}}$; (c) $\alpha_{\text{H}_2/\text{CH}_4}$; (d) $\alpha_{\text{H}_2/\text{CO}_2}$.



It appears clear that, in all analyzed cases, the ideal selectivity of hydrogen with respect to other gases is decreased by increasing the trans-membrane pressure. This behavior can be explained by taking into account the possible permeation mechanisms of each gas through the membrane. In particular, for He, N₂, CO₂ and CH₄, it has been observed that the permeating flux of each gas, taking place by Knudsen diffusion and viscous flow through the defects [40], is increased almost linearly by increasing the trans-membrane pressure. On the contrary, hydrogen permeates mainly by a solution-diffusion mechanism and its flux depends on pressure with a factor equal to 0.55 for the Pd/PSS and 0.54 for the Pd/Al₂O₃ membrane. Consequently, with rising pressure the increment of the permeating flux of each gas (He, N₂, CH₄ and CO₂) is higher than that of hydrogen. As a result, the ideal selectivity of hydrogen decreases with increasing trans-membrane pressure.

The H₂/N₂ and H₂/He ideal selectivities illustrated in Figure 6a,b were evaluated at the beginning of the experimental campaign, showing that the Pd/PSS membrane is characterized by higher ideal selectivities than Pd/Al₂O₃ membrane. On the contrary, the H₂/CH₄ and H₂/CO₂ ideal selectivities have been calculated after temperature variations, from 380 to 420 °C for Pd/PSS membrane and from 350 °C to 450 °C for Pd/Al₂O₃ one. Therefore, from Figure 6c,d, it is evident that there has been a deterioration of both membranes with respect to what reported in Figure 6a,b. In particular, the loss of performance in terms of ideal selectivity for the Pd/PSS membrane is shown to be larger than for the Pd/Al₂O₃ membrane.

In Table 3, the Pd/PSS and Pd/Al₂O₃ performance in terms of hydrogen flux, permeance and H₂/N₂ ideal selectivity are compared with similar data taken from the open literature.

Table 3. Comparison with scientific literature data.

Membrane type	Preparation method	Pd layer (μm)	T ($^{\circ}\text{C}$)	Δp (Pa)	H_2 flux ($\text{mol/s}\cdot\text{m}^2$)	H_2 permeance ($\text{mol/s}\cdot\text{m}^2\cdot\text{Pa}$)	$\alpha(\text{H}_2/\text{N}_2)$ (–)	References
Pd/CeO ₂ /PSS	ELP-CVD	6	500	100,000	0.235	–	14 ^b	[50]
Pd/ γ -Al ₂ O ₃ /Al ₂ O ₃	ELP	5	300	400,000	–	1.4×10^{-6}	1000	[51]
Pd/ZrO ₂ /PSS	ELP	23	400	100,000	0.0734	$5.2 \times 10^{-4\text{a}}$	320	[5]
Pd/ γ -Al ₂ O ₃ /Al ₂ O ₃	ELP	2.4	500	100,000	–	3.9×10^{-6}	32,500	[52]
Pd/Ni-SiO ₂ /PSS	CVD	–	450	42,000	–	6.4×10^{-6}	6100	[53]
Pd/YSZ/PSS	ELP	28	450	30,000–40,000	0.01–0.06	$4.5 \times 10^{-4\text{a}}$	∞	[54]
Pd/ γ -Al ₂ O ₃ /Al ₂ O ₃	ELP	2.6	370	400,000	–	4.8×10^{-7}	3000	[33]
Pd/ γ -Al ₂ O ₃ /Al ₂ O ₃	ELP	1	400	75,000	–	6.7×10^{-6}	23	[55]
Pd/SiO ₂ /PSS	CVD	6	500	50,000	0.133	2.7×10^{-6}	450	[46]
Pd/Al ₂ O ₃	CVD	2	300	30,000	–	3.3×10^{-6}	5000	[56]
Pd/Fe ₂ O ₃ /PSS	ELP	22	450	100,000	0.0853	$2.7 \times 10^{-4\text{a}}$	∞	[13]
Pd/ γ -Al ₂ O ₃ /Al ₂ O ₃	ELP	6	480	100,000	–	2.6×10^{-6}	2100 ^b	[31]
Pd/Al ₂ O ₃	CVD	1	450	68,000	–	2.1×10^{-6}	780	[28]
Pd/Al ₂ O ₃	ELP	0.9	460	199,000	–	3.1×10^{-6}	1200	[36]
Pd/PSS	ELP	20	350	100,000	–	5×10^{-7}	5000	[40]
Pd/NaAZ/PSS	ELP	19	450	50,000	0.0790	$1.1 \times 10^{-3\text{a}}$	608	[57]
Pd/PSS	ELP	10	400	200,000	0.176	8.7×10^{-7}	11,800	This work
Pd/Al ₂ O ₃	ELP	7	400	100,000	0.233	2.3×10^{-6}	7500	This work

^a this value is given in $\text{mol/s}\cdot\text{m}^2\cdot\text{Pa}^{0.5}$; ^b H_2/Ar Ideal Selectivity.

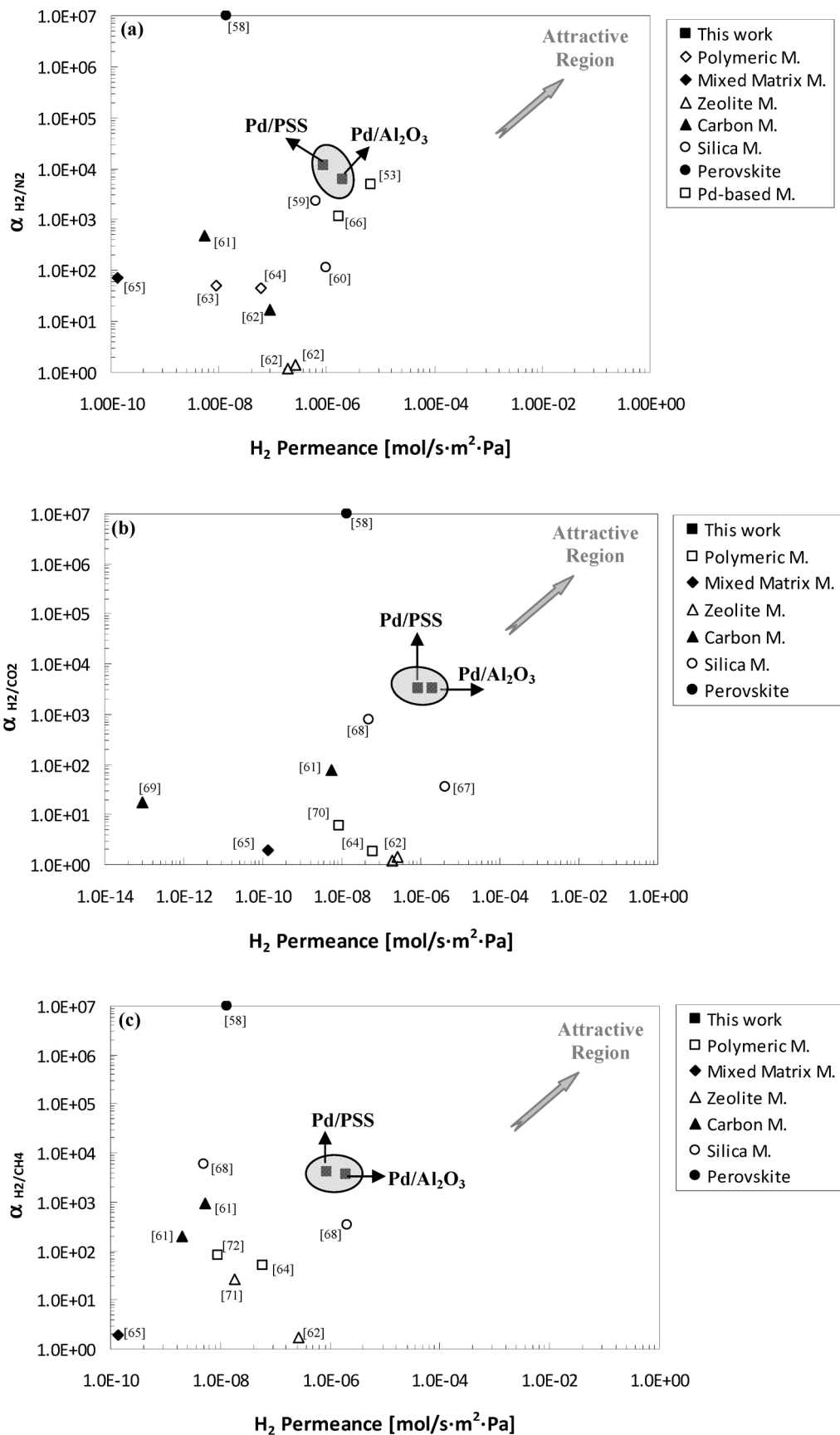
A rigorous quantitative comparison is quite difficult to carry out owing to the many different parameters involved such as the preparation method, Pd-layer, membrane type as well as the operating conditions (temperature and pressure range). From a qualitative point of view, it is evident that membranes, characterized by a thinner Pd-layer, show higher hydrogen permeating fluxes; nevertheless, their H_2/N_2 ideal selectivity is far from the ideal value of infinite, probably because of the presence of pinholes or defects. On the contrary, membranes having a thicker Pd-layer present lower hydrogen permeating flux but higher ideal selectivity. In particular, the membranes produced by Rothenberger *et al.* [13] exhibited an infinite ideal selectivity, working at ~ 0.3 bar as trans-membrane pressure. Nevertheless, these authors stated that this ideal-selectivity is not ensured at higher pressure. Indeed, when they increased the pressure from 5.0 to 28.0 bar, the ideal selectivity dropped from a value of 135 to 12.

However, as shown in Table 3 the performance of both Pd/PSS and Pd/Al₂O₃ membranes from this work are coherent with data from the open literature. In particular, the results indicate that both membranes present high hydrogen permeating fluxes and ideal selectivities.

As a further comparison, Figure 7a–c shows the ideal selectivity of H_2/N_2 , H_2/CO_2 and H_2/CH_4 against hydrogen permeance. In particular, the performance of the membranes of this work were compared to literature data obtained by using other kind of membranes such as polymeric, silica, carbon, mixed matrix and zeolite.

As well known, a trade-off exists between permeance and selectivity. Indeed, more permeable membranes are generally less selective and *vice versa*. In this contest, the efforts of research are devoted to produce membranes highly permeable and selective towards H_2 .

Figure 7. Comparison with scientific data. (a) α_{H_2/N_2} ; (b) α_{H_2/CO_2} ; and (c) α_{H_2/CH_4} vs. H_2 Permeance [53,58–72].

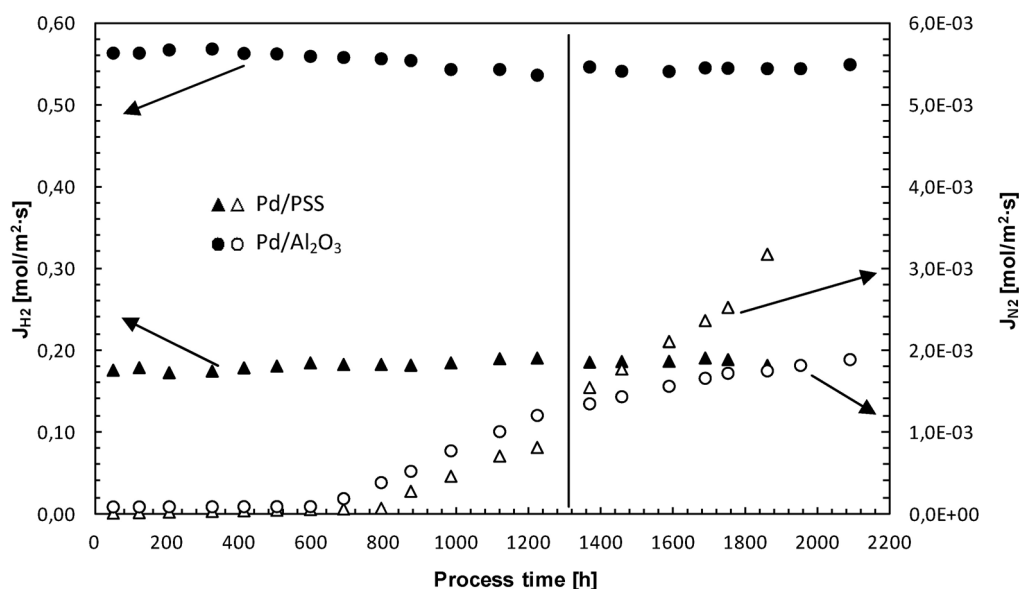


By referring to Figure 7a–c, the best performance are expected in the upper right hand corner. It is evident that both the Pd/PSS and Pd/Al₂O₃ membranes studied in this work showed a good compromise between ideal selectivity and H₂ permeance with respect to other referenced membranes. For instance, perovskite membranes [58] present very high ideal selectivity but low H₂ permeance working at high temperature. An opposite trend is shown by zeolite membranes, while comparable results to Pd-based membranes of this work were realized by using silica membranes [59,68]. Nevertheless, the CVD technique used for manufacturing these membranes is quite expensive.

3.4. Membrane Long-Term Stability and Life Time Estimation

The long-term H₂ permeance and H₂/N₂ ideal selectivity stability of Pd-based composite membranes represent an important key point for their real commercial application. Therefore, long-term stability tests were carried out by monitoring both composite membranes over a period of around 2000 h through permeation measurements with H₂ and N₂. At 400 °C and $\Delta p = 200$ kPa, H₂ and N₂ permeating fluxes through both Pd/PSS and Pd/Al₂O₃ membranes are given as a function of process time, Figure 8.

Figure 8. H₂ and N₂ permeating flux through both Pd/PSS and Pd/Al₂O₃ membranes as a function of process time.



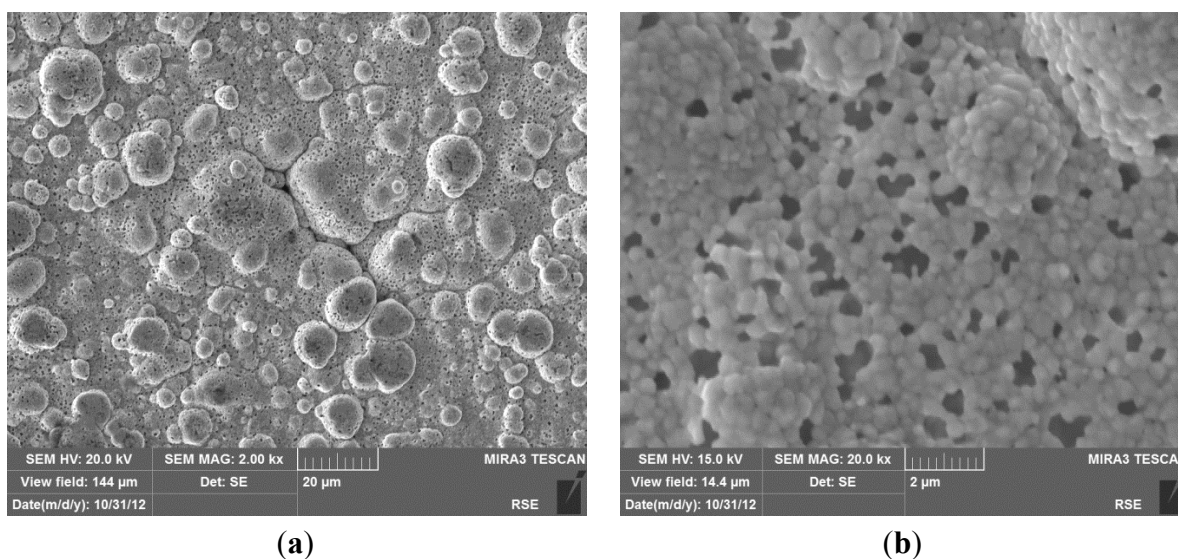
It is evident that hydrogen permeating flux through both membranes can be considered relatively stable for long-time operation under different operating conditions.

Concerning the N₂ flux, it can be considered constant up to 600 h and, then, increases progressively as a function of time. Up to 600 h, the operating temperature was kept constant at 400 °C. Successively, for performing permeation tests, it was varied from 380 to 420 °C for the Pd/PSS membrane and from 350 to 450 °C for the Pd/Al₂O₃ membrane. This temperature variation probably caused some changes in both Pd-based membrane structures [13,73]. In particular, as reported by Guazzone and Ma [73], it is possible that, at 400–450 °C, new pinholes could be formed owing to the sintering of small Pd clusters. More recently, Augustine *et al.* [74] evaluated the long-term stability of various Pd/PSS

membranes, also in the presence of steam and synthetic WGS mixture at 400–450 °C. These authors noticed that, although a decrease of selectivity was evidenced during the time, final values remained rather high (above 1000). In this work, however, the H₂/N₂ ideal selectivity of the Pd/PSS membrane dropped from 11700 to 55 after 1800 h of operating time, while it decreased from 6200 to 310 after 2100 h for Pd/Al₂O₃. The dramatic decrease of H₂/N₂ ideal selectivity for the Pd/PSS membrane could be attributed to the presence of some contaminants, rather than to the growth of pre-existing pinholes.

To investigate the causes of membrane degradation, the Pd/PSS membrane was analyzed by Scanning Electron Microscope (SEM). SEM images of the membrane surface are shown in Figure 9, which highlight the characteristic cauliflower morphology of Pd-clusters and the presence of pinholes on the whole surface, up to micron size. The formation of new pinholes in the palladium layer was probably determined by sulphur release from graphite seals, as previously investigated by the same authors utilizing a twin Pd/PSS membrane used in this work [75].

Figure 9. SEM images with secondary electrons of the Pd/PSS membrane surface at the end of the tests. (a) Typical morphology of Pd-clusters; (b) Presence of pinholes on the Pd-surface.



4. Conclusions

Two composite membranes, Pd/PSS and Pd/Al₂O₃, constituted by thin palladium layers deposited onto porous supports via ELP have been studied in the temperature range of 350–450 °C and from 100 to 800 kPa as retentate pressure.

The experimental measurements illustrated that, at 400 °C, both types of membranes showed interesting H₂/other gases ideal selectivities and hydrogen flux combined to long-term stability up to 600 h. Nevertheless, when the temperature was varied H₂/N₂ ideal selectivity decreased as a function of process time. In particular, H₂/N₂ ideal selectivity of the Pd/PSS membrane dropped from 11700 to 55 after 1800 h, whereas it decreased from 6200 to 310 after 2100 h for the Pd/Al₂O₃ membrane. This decrease was attributed for the Pd/PSS membrane to the formation of new pinholes in the palladium layer determined by sulphur release from graphite seals that, most likely, contributed to the degradation of both membranes.

Acknowledgments

The authors would like to thank the European Union's Seventh Framework Programme (FP/2007-2013) for the Fuel Cells and Hydrogen Joint Technology Initiative under grant agreement No. (303476) 10 due to the funding received for part of this work. Furthermore, it is acknowledged the research funds from the Italian Electrical System-Contract Agreement between RSE S.p.A. and the Ministry of Economic Development-for funding the Pd/PSS membrane testing of this work.

Author Contributions

Angelo Basile, leader of the group and corresponding author, directed the research activities relative to the contents of this manuscript; Simona Liguori was the principal investigator for this research activities; Adolfo Iulianelli collaborated in the aforementioned research activities and participated on the manuscript preparation; Francesco Dalena participated to the research activities of this manuscript; Pietro Pinacci was the leader of the group concerning the preparation of Pd/PSS membrane; Maria Broglia prepared the Pd/PSS membrane; Francesca Drago collaborated on the experimental activities made on Pd/PSS membrane; Yan Huang was the leader for the preparation of Pd/Al₂O₃ membrane.

Conflicts of Interest

The authors declare no conflict of interest.

References

1. Zornoza, B.; Casado, C.; Navajas, A. Advances in hydrogen separation and purification with membrane technology. In *Renewable Hydrogen Technologies-Production, Purification, Storage, Applications and Safety*; Gandia, L.M., Arzamendi, G., Dieguez, P.M., Eds.; Elsevier: Amsterdam, The Netherlands, 2013; Chapter 11, pp. 245–268.
2. Iulianelli, A.; Liguori, S.; Longo, T.; Basile, A. Inorganic Membrane and Membrane Reactor Technologies for Hydrogen Production. In *Hydrogen Production: Prospects and Processes*; Honery, D.R., Moriarty, P., Eds.; Energy Science, Engineering and Technology Nova Science Publishers, Series: Victoria, Australia, 2012; Chapter 12, pp. 377–398.
3. Basile, A.; Iulianelli, A.; Longo, T.; Liguori, S.; de Falco, M. Pd-Based Selective Membrane State of the Art. In *Membrane Reactors for Hydrogen Production*; Marrelli, L., de Falco, M., Iaquaniello, G., Eds.; Springer: New York, NY, USA, 2011; Chapter 2, pp. 21–55.
4. Hu, X.; Chen, W.; Huang, Y. Fabrication of Pd/ceramic membranes for hydrogen separation based on low-cost macroporous ceramics with pencil coating. *Int. J. Hydrog. Energy* **2010**, *35*, 7803–7808.
5. Huang, Y.; Dittmeyer, R. Preparation of thin palladium membranes on a porous support with rough surface. *J. Membr. Sci.* **2007**, *302*, 160–170.
6. Paglieri, S.N.; Foo, K.Y.; Way, J.D.; Collins, J.P.; Harper-Nixon, D.L. A new preparation technique for Pd/alumina membranes with enhanced high temperature stability. *Ind. Eng. Chem. Res.* **1999**, *38*, 1925–1936.

7. Li, A.W.; Grace, J.R.; Lim, C.J. Preparation of thin Pd-based composite membrane on planar metallic substrate part II. Preparation of membranes by electroless plating and characterization. *J. Membr. Sci.* **2007**, *306*, 159–165.
8. Yeung, K.L.; Sebastian, J.M.; Varma, A. Novel preparation of Pd/Vycor composite membranes. *Catal. Today* **1995**, *25*, 231–236.
9. Altinisik, O.; Dogan, M.; Dogu, G. Preparation and characterization of palladium-plated porous glass for hydrogen enrichment. *Catal. Today* **2005**, *105*, 641–646.
10. Zhang, K.; Gao, H.Y.; Rui, Z.B.; Liu, P.; Li, Y.D.; Lin, Y.S. High temperature stability of palladium membranes on porous metal supports with different intermediate layers. *Ind. Eng. Chem. Res.* **2009**, *48*, 1880–1886.
11. Kitiwan, M.; Atong, D. Effects of porous alumina support and plating time on electroless plating of palladium membrane. *J. Mater. Sci. Technol.* **2010**, *26*, 1148–1152.
12. Li, A.; Liang, W.; Hughes, R. Characterization and permeation of palladium/stainless steel composite membranes. *J. Membr. Sci.* **1998**, *149*, 259–268.
13. Rothenberger, K.S.; Cugini, A.V.; Howard, B.H.; Killmeyer, R.P.; Ciocco, M.V.; Morreale, B.D.; Enick, R.M.; Bustamante, F.; Mardilovich, I.P.; Ma, Y.H. High pressure hydrogen permeance of porous stainless steel coated with a thin palladium film via electroless plating. *J. Membr. Sci.* **2004**, *244*, 55–68.
14. Chen, S.C.; Tu, G.C.; Caryat, C.Y.; Hung, C.A.; Rei, M.H. Preparation of palladium membrane by electroplating on AISI 316L porous stainless steel supports and its use for methanol steam reformer. *J. Membr. Sci.* **2008**, *314*, 5–14.
15. Huang, Y.; Dittmeyer, R. Preparation and characterization of composite palladium membranes on sinter-metal supports with a ceramic barrier against intermetallic diffusion. *J. Membr. Sci.* **2006**, *282*, 296–310.
16. Shu, J.; Adnot, A.; Grandjean, B.P.A.; Kaliaguine, S. Structurally stable composite Pd–Ag alloy membranes: Introduction of a diffusion barrier. *Thin Solid Films* **1996**, *286*, 72–79.
17. Nam, S.E.; Lee, K.H. Hydrogen separation by Pd alloy composite membranes: Introduction of diffusion barrier. *J. Membr. Sci.* **2001**, *192*, 177–185.
18. Ma, Y.H.; Mardilovich, I.P.; She, Y. Hydrogen Gas-Extraction Module and Method of Fabrication. U.S. Patent 6,152,987, November 28, 2000.
19. Wei, L.; Yu, J.; Hu, X.; Huang, Y. Fabrication of H₂-permeable palladium membranes based on pencil-coated porous stainless steel substrate. *Int. J. Hydrog. Energy* **2012**, *37*, 13007–13012.
20. Chen, W.; Hu, X.; Wang, R.; Huang, Y. On the assembling of Pd/ceramic composite membranes for hydrogen separation. *Sep. Purif. Technol.* **2010**, *72*, 92–97.
21. Ahmad, A.L.; Mustafa, N.N.N. Sol-gel synthesized of nano composite palladium-alumina ceramic membrane for H₂ permeability: Preparation and characterization. *Int. J. Hydrog. Energy* **2007**, *32*, 2010–2021.
22. Hu, X.; Yu, J.; Song, J.; Wang, X.; Huang, Y. Toward low-cost Pd/ceramic composite membranes for hydrogen separation: A case study on reuse of the recycled porous Al₂O₃ substrates in membrane fabrication. *Int. J. Hydrog. Energy* **2011**, *36*, 15794–15802.
23. Chi, Y.H.; Yen, P.S.; Jeng, M.S.; Ko, S.T.; Lee, T.C. Preparation of thin Pd membrane on porous stainless steel tubes modified by a two-step method. *Int. J. Hydrog. Energy* **2010**, *35*, 6303–6310.

24. Sari, R.; Yaakob, Z.; Ismail, M.; Daud, W.R.W.; Hakim, L. Palladium-alumina composite membrane for hydrogen separator fabricated by combined sol-gel, and electroless plating technique. *Ceram. Int.* **2013**, *39*, 3211–3219.
25. Checchetto, R.; Bazzanella, N.; Patton, B.; Miotello, A. Palladium membranes prepared by r.f. magnetron sputtering for hydrogen purification. *Surf. Coat. Technol.* **2004**, *177–178*, 73–79.
26. Li, Z.Y.; Maeda, H.; Kusakabe, K.; Morooka, S.; Anzai, H.; Akiyama, S. Preparation of palladium-silver alloy membranes for hydrogen separation by the spray pyrolysis method. *J. Membr. Sci.* **1993**, *78*, 247–254.
27. Yam, S.; Maeda, H.; Kusakabe, K.; Morooka, S. Thin palladium films formed in support pores by metal-organic chemical vapour deposition method and application to hydrogen separation. *Ind. Eng. Chem. Res.* **1994**, *33*, 616–622.
28. Jun, C.S.; Lee, K.H. Palladium and palladium alloy composite membranes prepared by metal-organic chemical vapour deposition method (cold-wall). *J. Membr. Sci.* **2000**, *176*, 121–130.
29. Broglia, M.; Pinacci, P.; Radaelli, M.; Bottino, A.; Capannelli, G.; Comite, A.; Vanacore, G.; Zani, M. Synthesis and characterization of Pd membranes on alumina-modified porous stainless steel supports. *Desalination* **2009**, *245*, 508–515.
30. Cheng, Y.S.; Yeung, K.L. Effects of electroless plating chemistry on the synthesis of palladium membranes. *J. Membr. Sci.* **2001**, *182*, 195–203.
31. Zhang, X.; Xiong, G.; Yang, W. A modified electroless plating technique for thin dense palladium composite membranes with enhanced stability. *J. Membr. Sci.* **2008**, *314*, 67–84.
32. Zhang, K.; Gao, H.; Rui, Z.; Lin, Y.; Li, Y. Preparation of thin palladium composite membranes and application to hydrogen/nitrogen separation. *Chin. J. Chem. Eng.* **2007**, *15*, 643–647.
33. Nair, B.K.R.; Choi, J.; Harold, M.P. Electroless plating and permeation features of Pd and Pd/Ag hollow fiber composite membranes. *J. Membr. Sci.* **2007**, *288*, 67–84.
34. Peters, T.A.; Tucho, W.M.; Ramachandran, A.; Stange, M.; Walmsley, J.C.; Holmestad, R.; Borg, A.; Bredesen, R. Thin Pd-23%Ag/stainless steel composite membranes: Long-term stability, life-time estimation and post-process characterization. *J. Membr. Sci.* **2009**, *326*, 572–581.
35. Kulprathipanja, A.; Alptekin, G.O.; Falconer, J.L.; Way, J.D. Effects of water gas shift gases on Pd–Cu alloy membrane surface morphology and separation properties. *Ind. Eng. Chem. Res.* **2004**, *43*, 4188–4198.
36. Yun, S.; Ko, J.H.; Oyama, S.T. Ultrathin palladium membranes prepared by a novel electric field assisted activation. *J. Membr. Sci.* **2011**, *369*, 482–489.
37. Pinacci, P.; Broglia, M.; Drago, F. Development of Pd Composite Membranes for Hydrogen Production in Membrane Reactors. In Proceedings of the European Fuel Cell (EFC), Rome, Italy, 14–16 December 2011.
38. Pinacci, P.; Broglia, M.; Valli, C.; Capannelli, G.; Comite, A. Evaluation of the water gas shift reaction in a palladium membrane reactor. *Catal. Today* **2010**, *156*, 165–172.
39. Collins, J.P.; Way, J.D. Preparation and characterization of a composite palladium-ceramic membrane. *Ind. Eng. Chem. Res.* **1993**, *32*, 3006–3013.
40. Mardilovich, P.P.; She, Y.; Ma, Y.H.; Rei, M.H. Defect-free palladium membranes on porous stainless-steel support. *AIChE J.* **1998**, *44*, 310–322.

41. Guazzone, F.; Engwall, E.E.; Ma, Y.H. Effect of surface activity, defects and mass transfer on hydrogen permeance and n -value in composite palladium-porous stainless steel membranes. *Catal. Today* **2006**, *118*, 24–31.
42. Wang, D.; Tong, J.; Xu, H.; Matsumura, Y. Preparation of palladium membrane over porous stainless steel tube modified with zirconium oxide. *Catal. Today* **2004**, *93–95*, 689–693.
43. Tong, J.; Matsumura, Y.; Suda, H.; Haraya, K. Thin and dense Pd/CeO₂/MPSS composite membrane for hydrogen separation and steam reforming of methane. *Sep. Purif. Technol.* **2005**, *46*, 1–10.
44. Zahedi, M.; Afra, B.; Mobarake, M.D.; Bahmani, M. Preparation of a Pd membrane on a WO₃ modified porous stainless steel for hydrogen separation. *J. Membr. Sci.* **2009**, *333*, 45–49.
45. Ilias, S.; Su, N.; Udo-Aka, U.I.; King, F.G. Application of electroless deposition thin film palladium composite membrane in hydrogen separation. *Sep. Sci. Technol.* **1997**, *32*, 487–504.
46. Su, C.; Jin, T.; Kuraoka, K. Thin palladium film supported on SiO₂-modified porous stainless steel for a high-hydrogen-flux membrane. *Ind. Eng. Chem. Res.* **2005**, *44*, 3053–3058.
47. Chen, H.; Chu, C.; Huang, T. Comprehensive characterization and permeation analysis of thin Pd/Al₂O₃ composite membranes prepared by suction-assisted electroless deposition. *Sep. Sci. Technol.* **2005**, *39*, 1461–1483.
48. Mardilovich, I.P.; Engwall, E.; Ma, Y.H. Dependence of hydrogen flux on the pore size and plating surface topology of asymmetric Pd-porous stainless steel membranes. *Desalination* **2002**, *144*, 85–89.
49. Sanz, R.; Calles, J.A.; Alique, D.; Furones, L. New synthesis method of Pd membranes over tubular PSS supports via “pore-plating” for hydrogen separation processes. *Int. J. Hydrog. Energy* **2012**, *37*, 18476–18485.
50. Tong, J.; Sua, C.; Kuraoka, K.; Suda, H.; Matsumura, Y. Preparation of thin Pd membrane on CeO₂-modified porous metal by a combined method of electroless plating and chemical vapor deposition. *J. Membr. Sci.* **2006**, *269*, 101–108.
51. Tanaka, D.A.P.; Tanco, M.A.L.; Okazaki, T.N.J.; Wakui, Y.; Mizukami, F.; Suzuki, T.M. Fabrication of hydrogen-permeable composite membranes packed with palladium nanoparticles. *Adv. Mater.* **2006**, *18*, 630–632.
52. Li, H.; Goldbach, A.; Li, W.; Xu, H. PdC formation in ultra-thin Pd membranes during separation of H₂/CO mixtures. *J. Membr. Sci.* **2007**, *299*, 130–137.
53. Lee, D.W.; Lee, Y.G.; Nam, S.E.; Ihm, S.K.; Lee, K.H. Study on the variation of morphology and separation behavior of the stainless steel supported membranes at high temperature. *J. Membr. Sci.* **2003**, *220*, 137–153.
54. Sanz, R.; Calles, J.A.; Alique, D.; Furones, L.; Ordonez, S.; Marin, P.; Corengia, P.; Fernandez, E. Preparation, testing and modelling of a hydrogen selective Pd/YSZ/SS composite membrane. *Int. J. Hydrog. Energy* **2011**, *36*, 15783–15793.
55. Zhao, H.B.; Pflanz, K.; Gu, J.H.; Li, A.W.; Stroh, N.; Brunner, H.; Xiong, G.X. Preparation of palladium composite membranes by modified electroless plating procedure. *J. Membr. Sci.* **1998**, *142*, 147–157.
56. Itoh, N.; Akiha, T.; Sato, T. Preparation of thin palladium composite membrane tube by a CVD technique and its hydrogen permselectivity. *Catal. Today* **2005**, *104*, 231–237.

57. Bosko, M.L.; Ojeda, F.; Lombardo, E.A.; Cornaglia, L.M. NaA zeolite as an effective diffusion barrier in composite Pd/PSS membranes. *J. Membr. Sci.* **2009**, *331*, 57–65.
58. Heidari, M.; Zamaniyan, A.; Kordi, A.S.; Babakhani, E.G.; Amanipour, M. Effect of sintering temperature on microstructure and hydrogen permeation properties of perovskite membrane. *J. Mater. Sci. Technol.* **2013**, *29*, 137–141.
59. Gopalakrishnan, S.; Yoshino, Y.; Nomura, M.; Nair, B.N.; Nakao, S.I. A hybrid processing method for high performance hydrogen-selective silica membranes. *J. Membr. Sci.* **2007**, *297*, 5–9.
60. Lee, D.W.; Lee, Y.G.; Nam, S.E.; Sea, B.; Lee, K.H. Preparation and characterization of SiO₂ composite membrane for purification of hydrogen from methanol steam reforming as an energy carrier system for PEMFC. *Sep. Purif. Technol.* **2003**, *32*, 45–50.
61. Lie, J.A.; Hagg, M.B. Carbon membranes from cellulose and metal loaded cellulose. *Carbon* **2005**, *43*, 2600–2607.
62. Separation Technology R&D Needs for Hydrogen Production in the Chemical and Petrochemical Industries. Available online: <http://www.rom-innovation.com/pdf/separation-need-in-chemical-2020-and-hydrogen.pdf> (accessed on 18 February 2014)
63. Wang, D.L.; Li, K.; Teo, W.K. Effects of temperature and pressure on gas permselectivity properties in asymmetric membranes. *J. Membr. Sci.* **1995**, *105*, 89–115.
64. Pinnau, I.; Toy, L.G. Gas and vapor transport properties of amorphous perfluorinated copolymer membranes based on 2,2-bistrifluoromethyl-4,5-difluoro-1,3-dioxole/tetrafluoroethylene. *J. Membr. Sci.* **1996**, *109*, 125–133.
65. Sen, D.; Kalipcilar, H.; Yilmaz, L. Development of zeolite filled polycarbonate mixed matrix gas separation membranes. *Desalination* **2006**, *200*, 222–224.
66. Wang, D.; Flanagan, T.B.; Shanahan, K.L. Permeation of Hydrogen through Pre-oxidized Pd Membranes in the absence and Presence of CO. *J. Alloys Compd.* **2004**, *372*, 158–164.
67. Pakizeh, M.; Omidkhah, M.R.; Zarringhalam, A. Synthesis and characterization of new silica membranes using template–sol–gel technology. *Int. J. Hydrog. Energy* **2007**, *32*, 1825–1836.
68. Gu, Y.; Oyama, S.T. Ultrathin, hydrogen-selective silica membranes deposited on alumina-graded structures prepared from size-controlled boehmite sols. *J. Membr. Sci.* **2007**, *306*, 216–227.
69. Hatori, H.; Takagi, H.; Yamada, Y. Gas separation properties of molecular sieving carbon membranes with nanopore channels. *Carbon* **2004**, *42*, 1169–1173.
70. Shaoa, L.; Low, B.T.; Chunga, T.S.; Greenberg, A.R. Polymeric membranes for the hydrogen economy: Contemporary approaches and prospects for the future. *J. Membr. Sci.* **2009**, *327*, 18–31.
71. Hong, M.; Li, S.; Falconer, J.L.; Noble, D.R. Hydrogen purification using a SAPO-34 membrane. *J. Membr. Sci.* **2008**, *307*, 277–283.
72. Li, Y.; Chung, T.S. Highly selective sulfonated polyethersulfone (SPES)-based membranes with transition metal counterions for hydrogen recovery and natural gas separation. *J. Membr. Sci.* **2008**, *308*, 128–135.
73. Guazzone, F.; Ma, Y.H. Leak growth mechanism in composite Pd membranes prepared by the electroless deposition method. *AIChE J.* **2008**, *54*, 487–492.
74. Augustine, A.S.; Mardilovich, I.P.; Kazantzis, N.K.; Ma, Y.H. Durability of PSS-supported Pd-membranes under mixed gas and water–gas shift conditions. *J. Membr. Sci.* **2012**, *415–416*, 213–220.

75. Pinacci, A.B.P.; Iulianelli, A.; Broglia, M.; Drago, F.; Liguori, S.; Longo, T.; Calabrò, V. Ethanol steam reforming reaction in a porous stainless steel supported palladium membrane reactor. *Int. J. Hydrog. Energy* **2011**, *36*, 2029–2037.

© 2014 by the authors; licensee MDPI, Basel, Switzerland. This article is an open access article distributed under the terms and conditions of the Creative Commons Attribution license (<http://creativecommons.org/licenses/by/3.0/>).